A MapReduce-like Deep Learning Model for the Depth Estimation of Periodontal Pockets

Yusuke Moriyama[1], Chonho Lee[2], Susumu Date[2], Yoichiro Kashiwagi[3], Yuki Narukawa[3], Kazunori Nozaki[4] and Shinya Murakami[3]

[1]*Graduate School of Information Science and Technology, Osaka University, Osaka, Japan*

[2]*Cybermedia Center, Osaka University, Osaka, Japan*

[3]*Graduate School of Dentistry, Osaka University, Osaka, Japan*

[4]*Osaka University Dental Hospital, Osaka, Japan*

Keywords: Periodontal Disease, Periodontal Pocket, Convolutional Neural Networks, Deep Learning, Object Detection.

Abstract: This paper explores the feasibility of diagnostic imaging using a deep learning-based model, applicable to periodontal disease, especially periodontal pocket screening. Having investigated conventional approaches, we find two difficulties to estimate the pocket depth of teeth from oral images. One is the feature extraction of Region of Interest (ROI), which is pocket region, caused by the small ROI, and another is tooth identification caused by the high heterogeneity of teeth (e.g., in size, shape, and color). We propose a MapReduce-like periodontal pocket depth estimation model that overcomes the difficulties. Specifically, a set of MapTasks is executed in parallel, each of which only focuses on one of the multiple views (e.g., front, left, right, etc.) of oral images and runs an object detection model to extract the high-resolution pocket region images. After a classifier estimates pocket depth from the extracted images, ReduceTasks aggregate the pocket depth with respect to each pocket. Experimental results show that the proposed model effectively works to achieve the estimation accuracy to 76.5 percent. Besides, we verify the practical feasibility of the proposed model with 91.7 percent accuracy under the condition that a screening test judges severe periodontitis (6 mm or more).

1 INTRODUCTION

Deep learning algorithms such as convolutional neural networks (CNN) (LeCun et al., 2015), have rapidly become a promising methodology for diagnostic imaging. This methodology can be used to automatically diagnose the presence of tuberculosis in chest radiographs (Ting et al., 2018), to detect macular degeneration from fundus images (Burlina et al., 2017), and to locate malignant melanoma in skin images (Esteva et al., 2017).

Such diagnostic imaging is also important in the field of dentistry due to increasing demands on dental health care. Periodontal disease is one of the most pervasive infections in the world and reported 80 percent adults are infected with. It is mainly caused of tooth loss by the chronic periodontal inflammation resulting in the destruction of tooth support tissues. Moreover, it has recently become apparent that the disease may be one of the risk factors of diabetes and stroke (Khader et al., 2006)(Wu et al., 2000). The disease progresses chronically over a number of years, so usually, patients have no clear symptom until pathological severe condition resulting in loosening or loss of teeth. To notice the disease in its early stages that the patients have rare subjective symptoms is effective for preventing the progression. An application that people easily self-check the risk of severity without imparting burdens enhances patient participation in dental consultations.

This paper explores the feasibility of diagnostic imaging applicable to periodontal disease. Specifically, we design a deep learning model to estimate the depth of periodontal pockets that dentists generally measures with a probe to examine the severity of periodontal disease.

In order to efficiently extract and study the disease conditions from the image, we focused on two data features, hierarchy and regression, observed in oral images. Hierarchy means that teeth are numbered 1 to 8 in the up and down, left and right, and there are

Moriyama, Y., Lee, C., Date, S., Kashiwagi, Y., Narukawa, Y., Nozaki, K. and Murakami, S.
A MapReduce-like Deep Learning Model for the Depth Estimation of Periodontal Pockets.
DOI: 10.5220/0007405703880395
In *Proceedings of the 12th International Joint Conference on Biomedical Engineering Systems and Technologies (BIOSTEC 2019)*, pages 388-395
ISBN: 978-989-758-353-7

6 measuring points in each tooth. Regression means that the 6 measurement points represent the state of the tooth, 1 to 8 teeth indicate the state of the jaw, and the four regions (upper left, upper right, downer left and downer right) represent the oral cavity.

Due to the complex features of the data observed in oral images, the required accuracy can not be obtained by merely using the image recognition algorithm. In fact, as a preliminary investigation, we have trained a conventional CNN model on oral images. However, the estimation accuracy was around 44 percent. There is a need to implement a model to learn the periodontal disease condition consisting of two features collectively.

Besides, we looked at two difficulties leading to such low accuracy; a difficulty in the Region of Interest (ROI) extraction caused by small pocket region images, and a difficulty in tooth identification caused by a high heterogeneity among teeth.

Based on the lessons learned from our preliminary investigation, we propose a MapReduce-like deep learning model that automatically assesses the severity of periodontal disease from oral images. It is a computational framework for data structures having the aforementioned features, and it overcomes the two difficulties. Specifically, the proposed model extracts pocket region images following tooth identification, processed in parallel with respect to each multiple view of oral images, and then estimates pocket depth from the extracted pocket region images.

This paper is structured as follows. Section 2 provides the prior knowledge on periodontal disease for further discussion later. Section 3 shows the preliminary results when applying a conventional CNN model, and then clarifies the two difficulties we tackle to improve the estimation accuracy. Section 4 describes the proposed MapReduce-like deep learning model. Section 5 shows the evaluation results to verify the effect of the proposed model. Section 6 presents related work and discusses future work.

2 PRIOR KNOWLEDGE ON PERIODONTAL DISEASE

Periodontal disease or Pyorrhea is a chronic inflammation affecting the gums surrounding the teeth. In its early stage called *Gingivitis*, the gums become swollen and may bleed. In an advanced stage of gingivitis called *Periodontitis*, the teeth can become detached from the gums and loosen.

Generally and traditionally, dentists examine the severity of periodontal disease by measuring the depth of *periodontal pockets* for all teeth using a

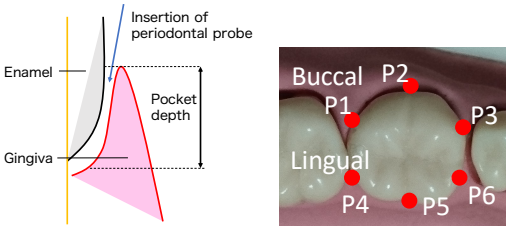

Figure 1: Illustration of periodontal pocket measurement (left) and 6 point measuring point (right).

probe (Figure 1-left). The measured depth is recorded in millimeters as a pocket chart. Under a common 6-point method, dentists measure six pockets: the distal buccal (P1), central buccal (P2), medial buccal (P3), medial lingual (P4), central lingual (P5), and distal lingual (P6) (Yoshie et al., 2013), as illustrated in Figure 1-right. In this paper, P1∼P6 are called pocket numbers and the gum region surrounding the pockets is called the *pocket region*.

In this paper, we define tooth number with three letters, for example, as in UL1 and DR8. The first letter is U or D for upper and downer, the second letter is L or R for left and right from the patient's view, and the third letter indicates the number from the median, respectively. For example, if the tooth number is UL1, UL1 represents the first tooth from the median in the upper left of the patient.

3 PRELIMINARY INVESTIGATION

To investigate the feasibility of applying deep learning techniques into the pocket depth estimation, we trained a conventional CNN model, called VGG-16 (Simonyan and Zisserman, 2014) with a set of oral images from 1333 patients acquired at the Osaka University Dental Hospital. The trained model estimates the depth of 12 pockets, which is the buccal side of 4 upper front teeth. Using 80 percent of the oral images as training, and 20 percent as the test, we observed the estimation accuracy of approximately 44 percent according to precision in millimeters.

In order to improve the accuracy, we have found ways to overcome the two difficulties in *Region of Interest (ROI) feature extraction* and *tooth identification*, which led to such low accuracy.

Difficulty in ROI Feature Extraction: The first problem is a small ROI in the oral image. According to dentists, the correlation between different pockets is weak even for the same teeth. So, for estimating a pocket depth, we better focus on the corresponding

pocket region. However, each pocket region is small in an oral image, and the "noise" unrelated to the estimation is large. Examples of the noise include teeth, lips, and other pocket regions. In addition, due to the high computational cost and large memory size, the input image size of the CNN model is limited in general. The size of the original oral image used in this study is large (e.g. 1600×1200 and 2080×1560), so it is necessary to reduce the image size to adjust to the size of model input. Therefore, as illustrated in Figure 2, if the entire oral image is the model input, the image resolution of ROI becomes lower than that of ROI in the original image.

Difficulty in Tooth Identification: The second problem is tooth heterogeneity. We focus on a pocket region to estimate a pocket depth, so we need to identify the corresponding teeth to extract the pocket region images. The training dataset contains a set of oral images taken from different directions for each of the patients. Depending on the direction, tooth features such as color, size and shape vary in those images even for the same teeth. In the case of general objects such as dog, cat, etc., that have large feature differences, the direction is not a problem. However, in the case of teeth, since the features are inherently similar, it becomes difficult to identify the teeth.

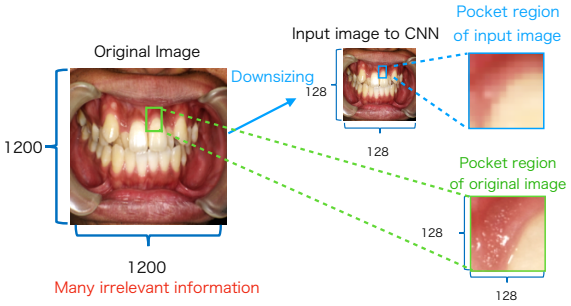

Figure 2: Quality of pocket region image (i.e., ROI). Note that we consider the CNN accepts a size of 128×128 input. The resolution of ROI input to the CNN is lower than that of ROI in the original image, and the information is lost.

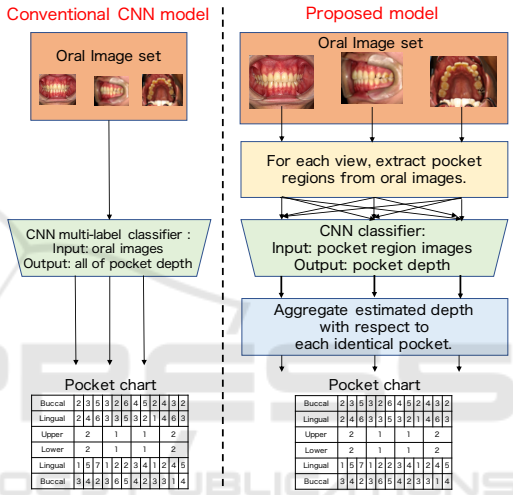

Figure 3: Overview flow of the pocket depth estimation.

4 DESCRIPTION OF THE PROPOSED MODEL

This section describes the proposed MapReduce-like periodontal pocket depth estimation model together with the design principles. Figure 3 illustrates the overview flow of the proposed model, where CNN pre-processing and post-processing are added. To overcome the first difficulty in ROI feature extraction, we extract high resolution pocket region images, provided to CNN. To overcome the second difficulty in tooth identification, we parallelize the pocket region extraction. The details of the process are explained in the following subsections.

4.1 Design Principles

First, we consider the extraction of pocket region images. To extract the pocket region images, we further need to identify tooth numbers which represent tooth location and pocket numbers, which represent the pocket location of the teeth. In order to identify the tooth numbers, we perform tooth detection first.

A few methods exist for the detection of teeth, such as image processing, segmentation, and object detection. In image processing, teeth can be detected, but it is difficult to classify tooth numbers. This is because the tooth numbers must be identified according to the coordinates of the detected teeth. However, image processing does not work when the alignment of the teeth is bad or the teeth are missing. The segmentation approach also is not suitable because when specifying tooth coordinates, this approach requires a contour acquisition process after pixel classification, which increases labor and processing time. For these reasons, we use object detection, named YOLOv2 (Redmon and Farhadi, 2017), which makes it possible to identify tooth numbers and acquire the coordinate of teeth. By obtaining teeth coordinates, we can extract sub-images of the pocket regions from the oral images based on the teeth coordinates.

Secondly, we parallelize the pocket region extraction process on the per-viewpoint of oral images. In other words, each pocket region extraction process uses oral images with one of the multiple viewpoints. This way of processing eliminates the necessity of learning tooth features in multiple directions with one

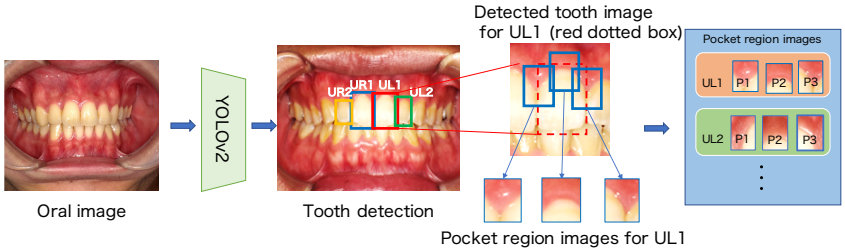

Figure 4: Pocket region extraction process (MapTask).

YOLOv2, and limits the range of tooth numbers. For example, in the oral image taken from the left direction, the right teeth are not included, so the classification can be limited to only the left teeth. As a result, we can reduce the misclassification of tooth numbers, which leads to an improvement in accuracy.

4.2 Design of the Proposed Model

In this subsection, we describe the proposed MapReduce-like periodontal pocket depth estimation model. The proposed model is divided mainly into three parts: the *Mapping* phase, the CNN phase, and the *Reducing* phase. The Mapping phase identifies tooth numbers and extracts pocket region images from oral images. The CNN phase estimates pocket depth from the pocket region images. The Reducing phase aggregates the estimated depth with respect to each identical pocket.

Mapping Phase: In this phase, a set of MapTasks that recognize teeth and extract pocket region images from oral images, is executed in parallel. Figure 4 shows our proposed pocket region extraction process that addresses the difficulty in ROI feature extraction. The process basically uses YOLOv2, known as a model capable of high-precision, high-speed object detection, to obtain the high resolution pocket region images.

YOLOv2 learns the features of each tooth so that it can detect the teeth and identify the tooth number, as illustrated in the red dotted box of Figure 4. Since three pocket regions exist at even intervals as shown in Figure 1-right, each of the detected tooth images is equally divided into three so as to correspond to those three pockets. Then, discarding the lower part of the tooth and including the gum, we can obtain the rectangular sub-images of pocket regions, which are a high resolution of large ROI images.

However, it is difficult for YOLOv2 to identify teeth with the same number (i.e., similar teeth such as upper front teeth, UL1 and UR1) because YOLOv2 recognizes objects by looking at features of size, color, and shape, but not its location. Therefore, in the case of the front view of the image, we compare the x-coordinate of the center of the detected rectangular to classify teeth into the left and right.

Each MapTask deals with one of the multiple viewpoints of oral images. Before parallelization, all oral images are input to the same MapTask. In the proposed method, the oral images are sorted in advance for each shooting direction and entered into the corresponding MapTask. Each MapTask extracts pocket region and passes them to the CNN phase.

CNN Phase: In this phase, the CNN classifier estimates pocket depth from the pocket region images. We use VGG-16 (Simonyan and Zisserman, 2014) pretrained by ImageNet. The CNN classifier takes an input image with the size of 128 $\times$ 128 and outputs one pocket depth with probability as the estimation confidence. Specifically, pocket region images extracted in the previous phase are sorted and grouped by tooth number and pocket number, as *identical pocket region* images. A group of identical pocket region images is input one by one to CNN classifier and outputs the group of estimated pocket depth.

Reducing Phase: In this phase, a set of ReduceTasks aggregates the estimated depth. Each ReduceTask handles one of the groups of pocket depth. There are a few ways to aggregate the pocket depth estimates with confidence. For example, the final pocket value is given as one pocket depth estimate with the highest confidence, or the weighted sum of the pocket depth estimate and confidence. In this paper, the former method is adopted. Figure 5 shows the detailed design of the proposed model.

5 EVALUATION

This section first explains the experimental environment and verifies the effects of the proposed model in terms of the estimation accuracy of pocket depth by comparing with that of a conventional CNN model.

Dataset: We use a dataset of 2625 oral images obtained from 1333 patients visiting at Osaka Univer-

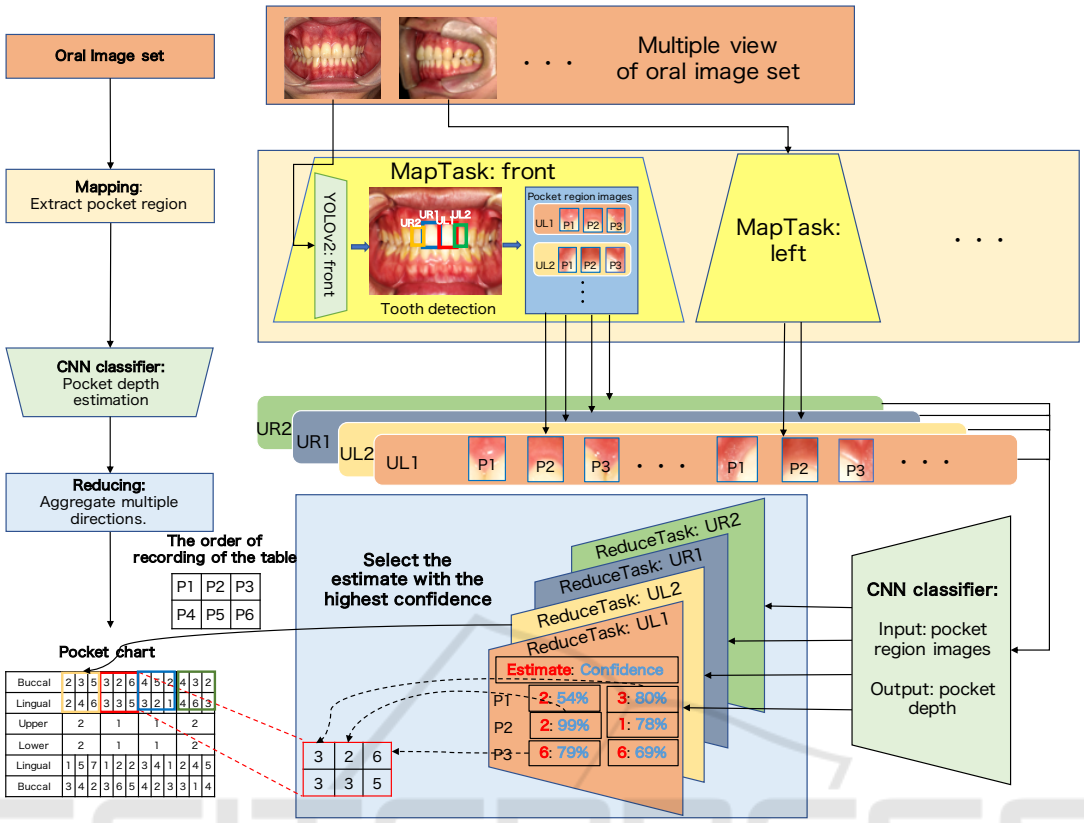

Figure 5: Design of the proposed model.

sity Dental Hospital. The images include ones taken from front and left directions. Data labels are the pocket depth of the teeth, which are measured by a few trained physicians. In this work, we focus on 12 pockets such as P1, P2, and P3 of teeth UL1, UL2, UR1 and UR2. The 80 percent of the data is used for training, and the remaining 20 percent is used for test.

Experimental Setting: The proposed model uses a CNN model, VGG-16, in its Reducing phase. The input image size is set to 128 × 128. To confirm feasibility according to usage, we change the number of classes of CNN based on pocket depth. We conduct three experiments as follows.

- E1: *Screening* by 2 stages, e.g., "Healthy" (3 mm or less) and "Unhealthy" (4 mm or more).
- E2: *Severity measurement* by 3 stages, e.g., "Healthy" (3 mm or less), "Moderate periodontitis" (4 or 5 mm), and " Severe periodontitis" (6 mm or more).
- E3: *Depth estimation* by 15 stages, i.e., pocket depth in millimeters between 1 mm and 15 mm.

In each experiment, we compare the proposed model with a single CNN model that outputs the estimates of 12 pocket depth at once. In order to perform multi-label classification, we parallelize final fully-connected layer of CNN. For example, in the case of Screening, the CNN has a 24 neurons (2 stages × 12 pockets) at final layer. For the evaluation metrics, we compute the classification accuracy, and mean-squared error (MSE) of the distance between the true pocket depth and the estimates.

5.1 Experimental Result

Table 2 shows the comparison result. It shows that the proposed model outperforms a single CNN model in the classification accuracy with an improvement of 1.2 percent at E1, 2.6 percent at E2, and 3.0 percent at E3, respectively. The accuracy improvement slightly increases as the number of classes increases. This indicates that the effect of the proposed MapReduce-like parallel processing becomes bigger against more complicated tasks.

In order to verify the effect, we conduct two additional experiments. The first experiment is to check how the image resolution of ROI (i.e., the pocket region image) affects accuracy, as shown in Figure 2. The second experiment is to check how the MapReduce-like task parallelization contributes to the improvement of accuracy.

Table 1: Pocket depth distribution of dataset consisting of 1333 patients, 2625 oral images and 15312 pocket regions. Note that the toothless part and the pocket without measurement data are deleted from the dataset.

Depth (mm)	1	2	3	4	5	6	7	8	9	10	11	12	13	14	15
The number of data	343	4702	6010	1442	504	654	218	101	104	35	34	4	1	1	0

Table 2: Accuracy (%) of pocket depth estimation using a single CNN and the proposed model (MSE (mm)).

Experiment	CNN	Proposed model
Screening	75.3 (0.25)	76.5 (0.21)
Severity measurement	70.5 (0.61)	73.1 (0.52)
Depth estimation	44.0 (2.20)	47.0 (2.14)

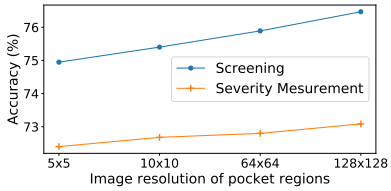

Figure 6: Accuracy over different image resolution of ROI.

5.1.1 Effect of Pocket Region Extraction

Different from a single CNN that learns oral images, the proposed model performs pocket region extraction and learns the pocket region images with less noise. In this experiment, we change the resolution of images to be input to CNN. Specifically, pocket region images of 64×64, 10×10, and 5×5 are used, respectively. This indicates that the images are magnified to 128×128, the input size of CNN.

Figure 6 shows the accuracy over different qualities of the pocket region images in the case of E1 and E2. As expected, the accuracy improves as the image resolution increases. This implies that the pocket region extraction contributes to improving the classification accuracy by focusing on a pocket region, which has a ROI with a higher resolution compared to the ROI in the oral image.

5.1.2 Effect of MapTask Parallelization

Different from a single CNN that learns both front and left views of oral images at once, the proposed model parallelizes tooth identification tasks, each of which deals only one-view image. In this experiment, the average precision (AP) of YOLOv2 is compared over

Table 3: Per-class average precision(%) and mean average precision(%) of YOLOv2. Note that UL1 and UR1 are represented as U1, and UL2 and UR2 are represented as U2.

View	AP of U1	AP of U2	mAP
Front	92.8	88.9	90.9
Left	79.0	77.6	78.3
Front + Left	62.6	62.3	62.5

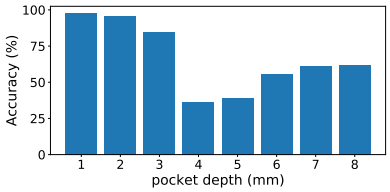

Figure 7: Accuracy over different pocket depth at E1.

different sets of oral images that contain a front view, left view, or both front and left views.

Table 3 shows the per-class AP and its mean (mAP). When the model uses both the front and left view images at once, the mAP decreases by more than 15 percent, compared with the case inputting one view image independently. Therefore, the MapTask parallelization is very effective.

Finally, we would like to discuss the low accuracy at Depth estimation (E3). The dramatic drop in accuracy could be caused by the unbiased dataset. The dataset includes a different number of oral images with different pocket depths, as shown in Table 1. It seems that the model was not trained well for the classes with large pocket depth because of the insufficient number of training data. To further improve the accuracy, we definitely need more data, i.e., oral images especially from patients with severe periodontal disease. Also, it would be beneficial to use other indices in addition to pocket depth such as the presence or absence of bleeding and blood sugar level to learn the relationship between oral images and the severity of periodontal disease.

5.2 Towards Practical Use

Although we verify the effect of pocket region extraction and parallelization, we need to further improve the estimation accuracy towards the practical periodontal screening. In this subsection, we show the result of an additional experiment to investigate the practical feasibility of periodontal screening with the proposed model.

Figure 7 shows the accuracy over different pocket depth at E1. As you can see, the accuracy of 4 and 5 mm is relatively lower than the others. We found that the pockets with 4 or 5 mm depth are wrongly classified as the pocket with 3 mm depth. In fact, it is also hard for dentists to judge the pockets with 4 or 5 mm depth (i.e., moderate periodontitis) from the

images, which do not have much visual difference. We doubt that pocket region images with ambiguous labels might be included in training dataset.

Thus, we consider ignoring the data (i.e., pocket region images) of 3, 4 and 5 mm pocket depth and see if the proposed model can be used for the *screening of severe periodontitis*, which differentiates "Healthy" (2 mm) from "Severe periodontitis" (6 mm or more). We named the experiment as E1′. If the pocket depth is more than 6 mm, the use of a surgical approach is likely to be necessary(Greenstein, 1997). Therefore, finding severe periodontitis is very important. Additionally, we ask a dentist to select data that he can distinguish whether it is severe in order to completely eliminate label ambiguity. That is, we perform E1′ on two different dataset as follows.

- E1′-a: A dataset of the pocket region images extracted by the Mapping phase of the proposed model (Healthy: 10449 images, Severe periodontitis: 2537 images).

- E1′-b: A dataset of the pocket region images the dentist selected from E1′-a dataset (Healthy: 1479 images, Severe periodontitis: 809 images).

Table 4 is the confusion matrix of E1′-a and E1′-b. From the results of E1′-a, the accuracy is 87.4 percent, true positive rate (TPR) is 93.3 percent, and false positive rate (FPR) is 29.7 percent. The accuracy improves compared to E1 case (76.5 percent), but FPR is so high that the model cannot be used for screening. From the results of E1′-b, the accuracy is 91.7 percent, TPR is 93.2 percent, and FPR is 6.8 percent. Compared to E1′-a model, the E1′-b model reduces FPR by approximately 20 percent.

Figure 8 compares ROC curves of E1 and E1′. From Figure 8, the area under the ROC curve (AUC) at E1′-a is 0.917 and the AUC at E1′-b is 0.962, which is approximately 0.2 larger than the AUC at E1. This implies that the E1′ makes less miss the case with high periodontal severity.

Through the experiments, we realize that there is not a strong relationship between pocket depth and the visual appearance of the pocket; especially the pockets with 4 mm or 5 mm depth (i.e., moderate periodontitis). However, the proposed model can judge severe periodontitis from pocket region images at over 91.7 percent accuracy with 6.8 percent FPR. As the results, we show the feasibility of screening for finding patients with severe periodontal disease. This will encourage people to do self-check at home and to see a doctor at right timing.

Table 4: Confusion matrix (E1′-a / E1′-b).

	Actual Healthy	Actual Severe periodontitis
Predicted Healthy	1806 / 206	201 / 18
Predicted Severe periodontitis	128 / 20	476 / 144

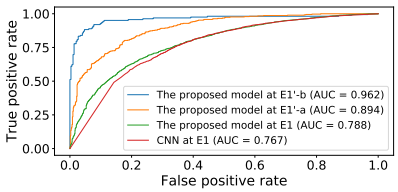

Figure 8: Comparison of ROC curves. Note that the threshold of the ROC curve uses the score for the Healthy class which is the output of CNN.

6 RELATED WORK AND FUTURE WORK

Related Work: Deep learning has been applied in various fields. One of the advantages in using deep learning is the ability to automatically extract effective and domain-specific features for tasks.

Deep learning has been applied in medical fields (Litjens et al., 2017) as well. Various models based on convolutional neural networks (CNN) have been proposed, which detect diabetic retinopathy from retinal fundus photographs (Gulshan et al., 2016), breast cancer in an mammography (Becker et al., 2017), and brain lesion segmentation in MRIs (Kamnitsas et al., 2017). Different from that type of research, our model parallelizes classification tasks, each of which only focuses on the corresponding ROI with less noise.

In the dental field, there are many studies related to the classification of dental diseases from X-ray images (Prajapati et al., 2017) and of dental plaque from quantitative light-induced fluorescence (QLF) images (Imangaliyev et al., 2016); however, few studies focuses on oral images. To the best of our knowledge, this study is the first study to investigate the relationship between oral images and pocket depth using deep learning.

Future Work: To further improve the estimation accuracy, the following work will be conducted.

First, we need to investigate the pocket regions around all teeth in addition to just the upper front teeth (e.g., UL1 and UR1). Different teeth and their pocket regions might have unique features that are different from those of the upper front teeth. As shown in Section 5.2.2, when we consider various teeth and more

images with multiple views, the effect of the proposed MapReduce like processing becomes much bigger.

Secondly, the proposed model mainly utilizes two trained models, YOLOv2 for tooth detection and CNN for pocket depth estimation. These models are independently trained on different set of images. We will try to design an end-to-end model by changing the current model's layer composition. This end-to-end model should be able to simultaneously train the model instantaneously.

Thirdly, in addition to the oral images, additional information such as X-ray images and blood test results should contribute to improving the estimation accuracy. We will work on designing a model that can handle a multimodal dataset.

7 CONCLUSION

In this paper, we proposed a MapReduce-like pocket depth estimation model which performed parallel pocket region extraction processing and multi-directional information aggregation in a Mapping phase and Reducing phase, respectively. Through the experiments, we realize that there is not a strong relationship between pocket depth and the visual appearance of the pocket. So, it is difficult to judge moderate periodontitis with only oral images. However, we show the feasibility of screening for finding patients with severe periodontal disease. The proposed model can be used for self-check at home as a tool with the same quality of vision as the dentists.

ACKNOWLEDGMENT

We would like to thank Osaka University Dental Hospital, for setting up the environment for our research and the medical dataset for the experiments. This work was supported by Social Smart Dental Hospital, a collaborative project between Osaka University and NEC Corp.

REFERENCES

Becker, A. S., Marcon, M., Ghafoor, S., Wurnig, M. C., Frauenfelder, T., and Boss, A. (2017). Deep learning in mammography: diagnostic accuracy of a multipurpose image analysis software in the detection of breast cancer. *Investigative radiology*, 52(7):434–440.

Burlina, P. M., Joshi, N., Pekala, M., Pacheco, K. D., Freund, D. E., and Bressler, N. M. (2017). Automated grading of age-related macular degeneration from color fundus images using deep convolutional neural networks. *JAMA ophthalmology*, 135(11):1170–1176.

Esteva, A., Kuprel, B., Novoa, R. A., Ko, J., Swetter, S. M., Blau, H. M., and Thrun, S. (2017). Dermatologist-level classification of skin cancer with deep neural networks. *Nature*, 542(7639):115.

Greenstein, G. (1997). Contemporary interpretation of probing depth assessments: Diagnostic and therapeutic implications. a literature review. *Journal of Periodontology*, 68(12):1194–1205.

Gulshan, V., Peng, L., Coram, M., Stumpe, M. C., Wu, D., Narayanaswamy, A., Venugopalan, S., Widner, K., Madams, T., Cuadros, J., et al. (2016). Development and validation of a deep learning algorithm for detection of diabetic retinopathy in retinal fundus photographs. *JAMA*, 316(22):2402–2410.

Imangaliyev, S., van der Veen, M. H., Volgenant, C. M., Keijser, B. J., Crielaard, W., and Levin, E. (2016). Deep learning for classification of dental plaque images. In *International Workshop on Machine Learning, Optimization and Big Data*, pages 407–410. Springer.

Kamnitsas, K., Ledig, C., Newcombe, V. F., Simpson, J. P., Kane, A. D., Menon, D. K., Rueckert, D., and Glocker, B. (2017). Efficient multi-scale 3d cnn with fully connected crf for accurate brain lesion segmentation. *Medical image analysis*, 36:61–78.

Khader, Y. S., Dauod, A. S., El-Qaderi, S. S., Alkafajei, A., and Batayha, W. Q. (2006). Periodontal status of diabetics compared with nondiabetics: a meta-analysis. *Journal of diabetes and its complications*, 20(1):59–68.

LeCun, Y., Bengio, Y., and Hinton, G. (2015). Deep learning. *nature*, 521(7553):436.

Litjens, G., Kooi, T., Bejnordi, B. E., Setio, A. A. A., Ciompi, F., Ghafoorian, M., van der Laak, J. A., van Ginneken, B., and Sánchez, C. I. (2017). A survey on deep learning in medical image analysis. *Medical image analysis*, 42:60–88.

Prajapati, S., Nagaraj, R., and Mitra, S. (2017). Classification of dental diseases u sing cnn and transfer learning. In *Proceedings of the 5th International Symposium on Computational and Business Intelligence (ISCBI)*.

Redmon, J. and Farhadi, A. (2017). YOLO9000: Better, faster, stronger. In *Proceedings of the 30th IEEE Conference on Computer Vision and Pattern Recognition*, pages 6517–6525.

Simonyan, K. and Zisserman, A. (2014). Very deep convolutional networks for large-scale image recognition. *arXiv preprint arXiv:1409.1556*.

Ting, D. S., Yi, P. H., and Hui, F. (2018). Clinical applicability of deep learning system in detecting tuberculosis with chest radiography. *Radiology*, 286(2):729.

Wu, T., Trevisan, M., Genco, R. J., Dorn, J. P., Falkner, K. L., and Sempos, C. T. (2000). Periodontal disease and risk of cerebrovascular disease: the first national health and nutrition examination survey and its follow-up study. *Archives of Internal Medicine*, 160(18):2749–2755.

Yoshie, H., Itou, K., Murakami, S., and Shin, K. (2013). *Clinical periodontal disease*. Ishiyaku Publishing, 2 edition.